OPEN

Paper

Effects of a Modified Chitosan Compound Combined with Lung Lavage after Inhalation of Depleted Uranium Dust

Yao Xiao,[1] Feng Zeng,[1] Weilin Fu,[1] Yi Zhang,[1] Xiangyu Chen,[1] Yi Liang,[2] Rong Li,[3] and Minghua Liu[1]

Abstract—**When exposed to depleted uranium (DU), the respiratory tract is the main route for DU to enter the body. At present, lung lavage is considered to be a method for removing DU from the lung. However, there is still room for improvement in the efficiency of lung lavage. In this work, a model of DU dust inhalation injury was established in beagle dogs so that chitosan-diethylenetriaminepentaacetic nanoparticles (CS-DTPA NP) could be synthesized. The purpose of this work was to evaluate the removal efficiency of CS-DTPA NP combined with lung lavage in dogs. Results showed that 7 d after DU exposure, the diethylenetriaminepentaacetic (DTPA) and CS-DTPA NP groups showed lower U content in kidney tissue compared with the normal saline (NS) group. In the left lung tissue (lavage fluid and recovery rate of lavage fluid), the U content in the CS-DTPA NP group was higher than in the NS and DTPA groups. In terms of blood levels, the CS-DPTA NP group increased over time at 1, 3 and 7 d of DU exposure without lavage; however, the U levels in the 3 and 7 d lavage groups were significantly lower than in the non-lavage groups. IL-1 in the lavage fluid of the CS-DPTA NP and CS NPs group were lower than in the NS group. In summary, after respiratory exposure to DU, early inhalation of CS-DPTA NP may block insoluble DU particles in the lung, and if combined with lung lavage, the clearance efficiency of DU from lung tissue improves.**

Health Phys. 122(6):663–672; 2022

Key words: aerosols; DTPA; kidneys; lungs; human

INTRODUCTION

Natural uranium consists of three radioisotopes: ^{238}U, ^{235}U and ^{234}U. Depleted uranium (DU) is a byproduct of the reaction of natural uranium into nuclear fuel. In contrast to natural uranium, DU has 70% less of ^{235}U but 99.8% of ^{238}U content, indicating lower radioactivity. Due to its high density and low radioactivity, it is widely used in heavy tank armors, armor-penetrating shells, missiles, and some civilian devices. DU has radiotoxicity and chemical toxicity effects in the human body, with the latter as the main effect. When DU weapons explode, a large amount of DU dust and aerosol particles would be produced. If this occurs at extremely high temperatures, uranium metal will oxidize into a series of composite oxides, including triuranium octaoxide (U_3O_8), uranium dioxide (UO_2), and uranium trioxide (UO_3) (Fulco et al. 2000; Priest 2001; Craft et al. 2004).

DU enters the body through skin shrapnel residue, ingestion, and inhalation, among which the respiratory tract is the main exposure route (Miller et al. 2017). The body absorption of DU varies according to concentration, shape, and particle size. Petitot et al. (2013) found that DU nanoparticles smaller than 100 nm could be rapidly absorbed and deposited in the respiratory tract of rats. A portion of DU entering the respiratory tract is flushed through the mucosal cilia and swallowed into the gastrointestinal tract before being excreted. It can also deposit in the lungs, especially in the insoluble form, and remain in the alveolar area before slowly dissolving (Craft et al. 2004; Yue et al. 2018). Therefore, accelerating the removal of insoluble DU aerosols, shortening the retention time, and reducing the concentration of DU aerosols in lung tissues will exert beneficial effects to human bodies (Gu et al. 2012).

Currently, chelating agents are used for the acute and chronic treatment of metal poisoning (Andersen 1999), among which diethylenetriaminepentaacetic acid (DTPA) is a broad-spectrum chelating agent recommended by the FDA for the decontamination or treatment of individuals exposed to radioactive elements and lanthanides (USFDA 2004; Cao et al.

[1]Emergency Department, The Southwest Hospital of Third Military Medical University, Chongqing, China; [2]Emergency Department, The General Hospital of Western Theater Command of PLA, Chengdu, China; [3]Institute of Combined Injury, College of Preventive Medicine, Third Military Medical University, Chongqing, China.

The authors declare no conflicts of interest.

For correspondence contact: Emergency Department, Southwest Hospital of the Third Military Medical University, 30, Gaotanyan Zheng Street, Shapingba District, Chongqing 400038, China, or email at **mhliuswhcq@126.com**.

(*Manuscript accepted* 20 *January* 2022)

0017-9078/22/0

DOI: 10.1097/HP.0000000000001557

2014; Yue et al. 2018). However, according to the results of actinide biodynamic experiments, the chelating agent must be able to pass through the cell membrane and reach where the radionuclide was distributed. Unfortunately, DTPA hardly passes through the cell membrane and can only target free radionuclides in the blood (Taylor 1983).

As one of the most abundant natural polysaccharides, chitosan (CS), or polyglucosamine (1–4) -2-amino-B-Dglucose has many advantages, including its lack of toxicity, biocompatibility, biodegradability, and bioactivity (Zhuang et al. 2020; Mikušová and Mikuš 2021). Due to the large number of amino and hydroxyl groups in chitosan, it can chelate heavy metal ions and is widely used as a biosorbent for polluted water (Zhang et al. 2017). Liu et al. (2012) linked water-soluble low molecular weight chitosan (WSC) to DTPA using a N-acetylation reaction and created WSC-DTPA nanoparticles, indicating that these nanoparticles enter cells through their membrane within 2 h. Hu et al. (2013) showed that WSC-DTPA nanoparticles promoted the excretion of DU in vivo, and the accumulation of DU in tissue cells was reduced by intravenously injecting uranyl nitrate into rats.

Chelating agents could be directly delivered to the lungs for better elimination of deposited radionuclides in the lungs. Inhalation therapy not only avoids first-pass metabolism by the liver but also shows high local drug concentrations and few systemic adverse effects (Bosquillon et al. 2001; Wang 2011). In addition, Ran et al. (2020) suggested that after exposure to DU, soluble uranium could be removed from the body using chelating agents, while the insoluble fraction of uranium could be removed using lung lavage. Dean et al. (1997) also suggested that lung lavage can be used to remove radionuclides. As a safe and relatively non-invasive method, lung lavage could be used to distinguish the deposited radionuclides from infections, diseases, and malignancies in lungs (Walters and Gardiner 1991). For insoluble radionuclide particles in the respiratory system, we have also demonstrated the effectiveness of lung lavage previously (Fu 2021).

However, there are no reports using nanoparticles in combination with lung lavage to treat respiratory exposure. Based on this, we synthesized CS-DPTA NP in this study based on the methods in prior studies (Hu 2013). A DU contamination model in beagle dogs was established using a modified microfiber bronchoscopy-guided spray bronchial device (Patent. No: CN201921851213.X). CS-DPTA NP was directly inhaled into the lung. Lung lavage was used to investigate the effects of CS-DPTA NP on the removal of insoluble DU particles in contaminated lungs.

MATERIALS AND METHODS

Synthesis and characterization of CS-DTPA

The CS-DTPA was prepared as described in previous studies (Hu 2013). Briefly, CS (DD = 92.3%, Mv = 3000, purchased from Nantong Xingcheng Biological Products Factory, Jiangsu, China) was added to 1% hydrochloric acid solution. The flask was mixed to fully dissolve the CS. DTPA (Shanghai Xinyu Biotechnology Co., Shanghai, China) was weighed at 20:1 and added into the CS solution and mixed using magnetic stirring. The pH of the solution was adjusted to 5–6 by NaOH solution. 1-(3-Dimethylaminopropyl)-3-ethylcarbodiimide hydrochloride (EDC; Aladdin) and N-hydroxysuccinimide (NHS, Aladdin) were added to the solution. Then, the solution was subjected to magnetic stirring for 24 h at 30 °C. At the end of the reaction, the solution was placed into dialysis bags and repeatedly purified with deionized water and sodium hydroxide solution for 3 d. Finally, the product was prepared by vacuum freeze-drying and stored at −20 °C.

Dried CS-DTPA were compressed into tablets using a KBr press. Fourier transform infrared spectroscopy (FTIR) was acquired using an iS10 FT-IR spectrometer within the scan range of 400–4,000 cm^{-1}. The spectrometer had a resolution of 4 cm^{-1}, signal-to-voltage ratio of 505:1, and 64 scans. The ^{1}H nuclear magnetic resonance (NMR) spectra of CS-DTPA were recorded on Agilent 600 MHz NMR (Agilent Technologies, Lexington, MA) spectrometer using deuterium oxide (D_2O).

Preparation of CS-DPTA NP

CS-DTPA nanoparticles were prepared using the ionic gelation method (López-León et al. 2005; Jhaveri et al. 2021). The appropriate amount of CS-DTPA was added to 1% acetic acid solution under magnetic stirring overnight. The concentration of CS-DTPA solution was 5 mg mL^{-1}, with the pH of the solution adjusted to 5–6 by 0.1 mol L^{-1} NaOH solution. Sodium tripolyphoshate (STPP) solution was added to the CS-DTPA solution under 800 ± 10 rpm stirring at room temperature for 30 min. The mass ratio of STPP solution to CS-DTPA solution was 3:1.

Characterization of CS-DPTA NP

The particle size of NPs was determined using a Zetasizer Nano (Malvern Panalytical, Ltd., 2000, Malvern, UK) at 25 ° C. Transmission electron microscopy (TEM) analysis was performed using a transmission electronic microscope (JEM-F200, Franklin, MA).

Animals

Thirty-two adult beagle dogs (50% male and 50% female), weighing 10.0 ± 1.8 kg, were provided by the Institute of Experimental Animals of Chongqing Academy of Traditional Chinese Medicine [Chongqing, China; Animal Certificate license No.: scxk (Su) 2018-0007]. All experiments were implemented in accordance with animal protection guidelines and approved by the Animal Ethics Committee of the Third Military Medical University.

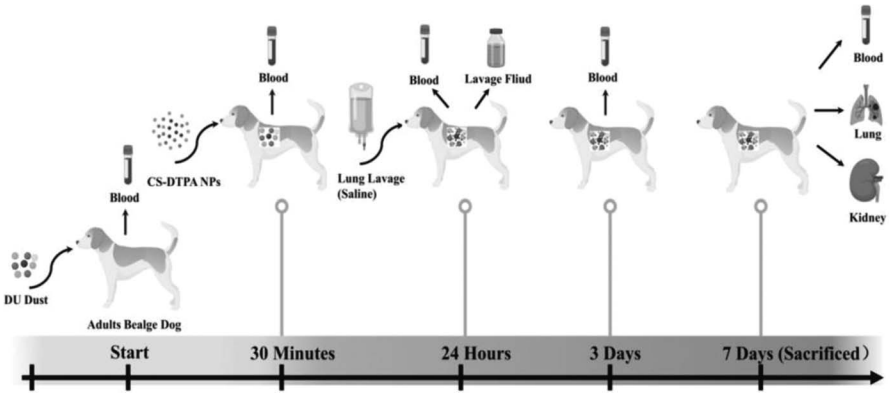

Fig. 1. Schematic illustration of model and treatment of lung contamination in beagle dogs.

Establishment of a model for acute lung injury by DU exposure and four intervention treatments

DU oxide powder (U_3O_8; National Munitions Corporation, Beijing, China) with a geometric diameter of 1–6 μm (average, 2.7 μm) was grounded, passed through a 500-mesh sieve, accurately weighed, sterilized under high pressure, mixed with normal saline into a 50 mg mL^{-1} suspension and continuously stirred at low speed using a magnetic agitator (MS7-H550-Pro, Yongli Instrument Co. LTD, Suzhou, China) (Zhang et al. 2011).

A model of DU dust inhalation injury in beagle dogs was established based on the literature (Fu et al. 2021) (Fig. 1). Each group was fasted for 12 h before the experiment. An intramuscular injection of serazine hydrochloride (approximately 1.5 mL) was administered to each dog based on their weight before DU exposure. Dogs were sent to the laboratory when anesthesia took effect. Dogs were placed in the supine position, with heads tilted back and limbs bound and fixed on the experiment table, followed by the insertion of a hand-held laryngoscope through the oral cavity. After provoking the epiglottis, a double-lumen bronchial intubation tube (32 Fr LEFT) was inserted into the left main bronchus through the laryngoscope. Under the guidance of an ultrafine fiberoptic bronchoscope, the front end of the catheter of the spray staining device designed by the research group was placed at the bifurcation of pulmonary lobar bronchi. The left chest of the dog was patted and injected with the DU suspension at a dose of 10 mg kg^{I-1}. After completion, the animals were quickly turned up and down for 3 min to make the DU suspension evenly distributed in the left lung tissue. After 30 min of exposure to DU, the four groups were treated with normal saline, DTPA, CS NPs, and CS-DPTA NP (30 mg kg^{-1}) through ultrasonic aerosol inhalation for 30 min. The endotracheal tube was removed once the dog woke up. All experiments were conducted in animal operating rooms with aseptic techniques.

The lung lavage procedure

The lung lavage procedure was performed consistently with that of the previous studies (Fu et al. 2021). Dogs were placed on operating tables and treated with lung lavage 24 h after DU exposure, with anesthesia induced through intramuscular injection of 3% pentobarbital sodium solution (0.8 mL kg^{-1}) during lung lavage. A ventilator [mode, intermittent positive-pressure ventilation (IPPV); fraction of inspired oxygen, 100%; tidal volume, 300–500 mL; respiratory frequency, 12–20 beats min^{-1}; inspiratory/expiratory ratio, 1:2] was connected to control the dog's ventilation mechanically for 5 min. The status of dogs was observed. If nothing unusual was observed, both lungs were ventilated with pure oxygen for 10 min to reserve oxygen.

Then, lung lavage treatment was performed on the left lung. The joint of the ventilation lung was connected to the catheter of the ventilator, while that of the endotracheal tube in the lavage lung was connected to a three-way lavage catheter. During each lavage, 20 mL kg^{-1} NS (maintained at a temperature of 37 °C) was perfused at a rate of 80 mL min^{-1} and retained in the lung for 1 min before being withdrawn at a rate of 160 mL min^{-1}. To increase the collected recovery of lavage fluid and reduce residual fluid in the lungs, dogs required chest clapping and negative pressure aspirators. An ultrafine fiberoptic bronchoscope was used to observe and quickly evaluate the lavage procedure to prevent the lateral leakage of lavage fluid caused by catheter movement during lung lavage. After the third lavage, the lung was ventilated for 3 min using an artificial balloon and then connected to a ventilator for 10 min of controlled ventilation with pure oxygen. After the dogs awoke, they were observed for reexpansion of both lungs and evidence that their vital signs (e.g., heart rate and respiration) were stable. Dogs were returned to the animal room after the lung lavage procedure.

Effect of CS-DPTA NP and lung lavage on U content

For U analysis, venous blood was collected from each group at 1, 3, and 7 d of DU exposure. Lavage fluid was recovered and fixed where 1.0–2.0 mL was taken to determine U content. This was then separated using a high-capacity centrifuge at 1,000 rpm (TDZ4-WS, Xiangyi Centrifuge Instrument Co. LTD, Changsha, China) for 5 min. Sediments were collected to determine U content in the lavage fluid.

In addition, dogs in each group were sacrificed after 7 d by injecting 10% Kcl solution into the heart cavity. The lung and kidneys were removed and fixed using a meat grinder (S18-LA527; Jiu Yang Co., Shangdong, China). Then, 1.0–2.0 g of lung tissues and kidney tissues were sent to determine U content. Determination of U was performed using inductively coupled plasma mass spectrometry (ICP-MS, ELEMENT XR, Thermo Fisher Scientific, Bremen, Germany).

L-1, TNF-α, and IL-10 levels in lavage fluid

A total of 5 mL of the recovered lavage fluid was centrifuged at 1,000 rpm for 5 min, and the supernatant was collected. The IL-1, TNF-α, and IL-10 levels in the lavage fluid were detected using an enzyme-linked immunosorbent assay, according to the manufacture's protocol (ELISA Shanghai Enzyme Link Biotechnology Co., Shanghai, China).

Pathological examination

Dogs were sacrificed 7 d after DU exposure. Lung tissue was fixed in 4% formaldehyde to prepare pathological sections following routine procedures. The specimens were stained with hematoxylin-eosin (H&E) and Masson staining before being examined using an optical microscope (He 2014). To evaluate tissue damage, inflammatory cell infiltration was semi-quantitatively scored by assessing random areas. The scoring criteria and methods were performed following previous work (Inal et al. 2014): 0 = No damage observed, 1 = 1 ~ 25%, 2 = 26 ~ 50%, 3 = 51 ~ 75%, 4 = 76 ~ 100%. The scoring was blinded and measured by a single pathologist using an Olympus BX51 microscope (Olympus, Tokyo, Japan). The mean scores (five areas per specimen) were averaged to yield a final score for each animal.

Statistical analysis

All experimental data were expressed as mean ± standard deviation (SD). The data of this study were processed using SPSS 25.0. One-way ANOVA followed by Dunnett's multiple comparisons test was performed using GraphPad Prism version 8.0.0 for Windows (GraphPad Software, San Diego, CA, www.graphpad.com., statistical software). The threshold P value was set at 0.05.

RESULTS

Characterization of CS-DTPA and CS-DPTA NP

As shown in Fig. 2, CS-DTPA was chemically synthesized using CS and DTPA. The successful synthesis of these conjugates was characterized by FTIR and ^{1}HNMR. In the FTIR for CS-DTPA (Fig. 3a), 1,631 cm^{-1} was the characteristic peak of the amide bond connected by n-acylation between $-NH_2$ on CS and $-$ COOH on DTPA, while 3,427 cm^{-1} and 1,391 cm^{-1} were the characteristic peaks of $-CH_2-$ and $-$ COO$-$ in CS-DTPA products, respectively. In summary, a CS-DTPA polymer was successfully prepared.

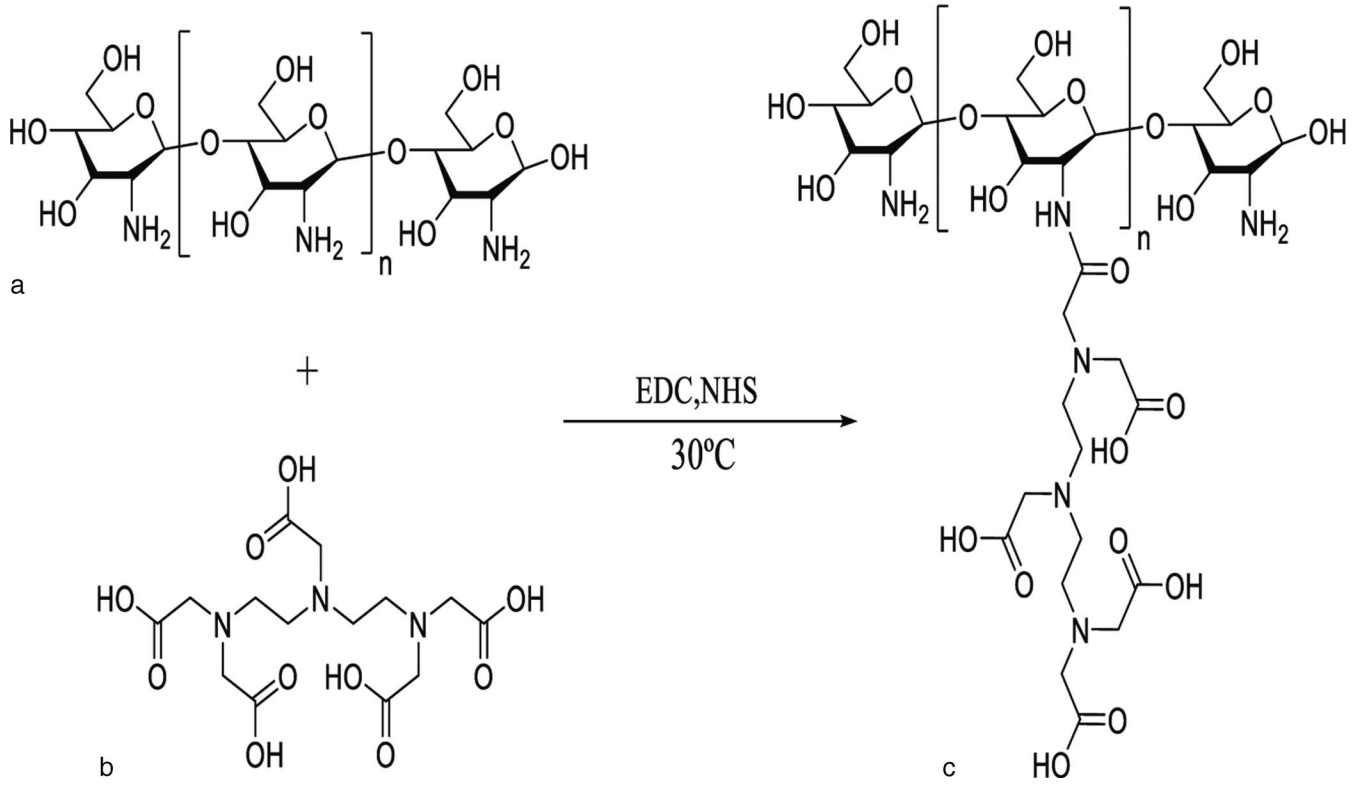

Fig. 2. Structures and synthesis route of chitosan-diethylenetriaminepentaacetic acid (CS-DTPA). (a) chitosan; (b) diethylenetriaminepentaacetic acid; (c) CS-DTPA.

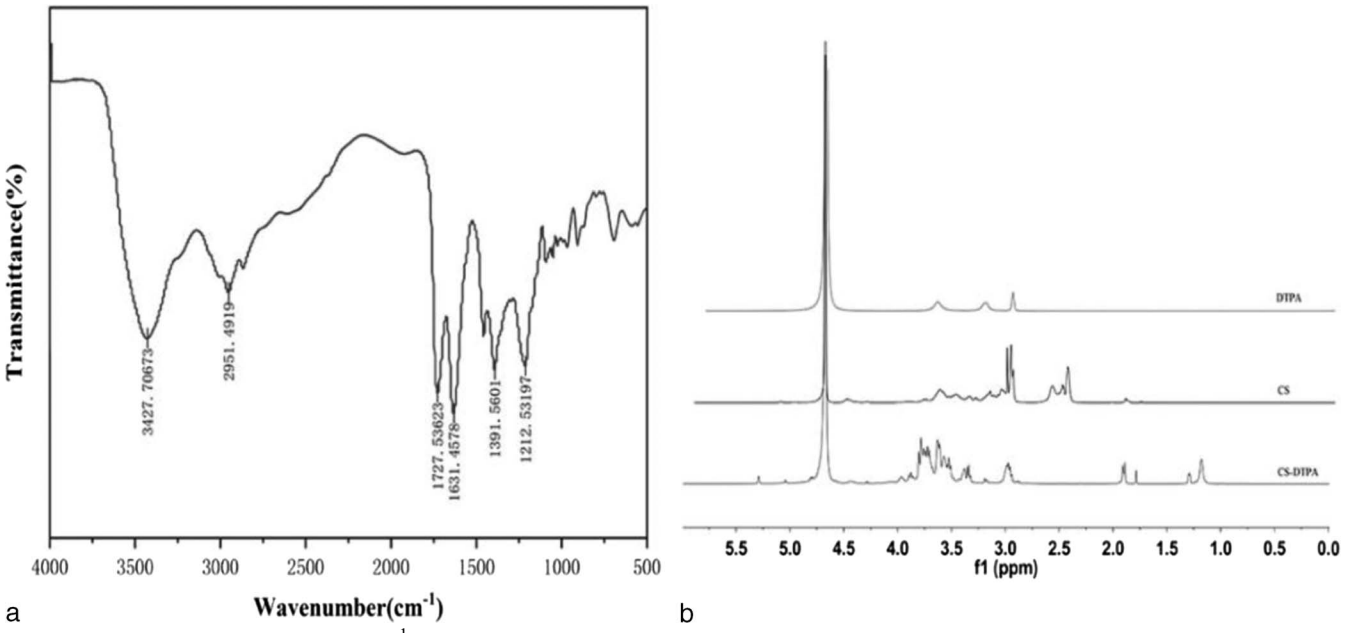

Fig. 3. (a) FTIR spectra of CS-DTPA; (b) ^{1}H nuclear magnetic resonance (NMR) of CS-DTPA.

Based on ^{1}H-NMR (Fig. 3b), δ4.8 was the solvent peak and δ2.5 was the H peak in $-NH_2$ on CS. Compared to the ^{1}H-NMR of CS, the peak between δ1.0 and 2.0 was the n-acylated amide bond between $-NH_2$ on CS and − COOH on DTPA. This indicated that DTPA was successfully grafted onto CS.

CS-DPTA NP were successfully prepared by ionotropic gelation. As for DLS (Fig. 4a), the nanoparticle size was 263.8 ± 54.1 nm, and the polydispersity (PDI) value was 0.157. PDI was less than 1, indicating that the nanoparticles were uniform and dispersed in solution (Hosseini et al. 2018). According to the TEM photograph (Fig. 4b), CS-DPTA NP showed that the nanoparticles were spherical with a uniform size and good dispersion, consistent with DLS results.

Effect of CS-DPTA NP and lung lavage on U content

Results (Fig. 5a) showed that, compared with the other three groups, the level of DU in the kidney tissues of the CS-DPTA NP group was significantly lower than the NS

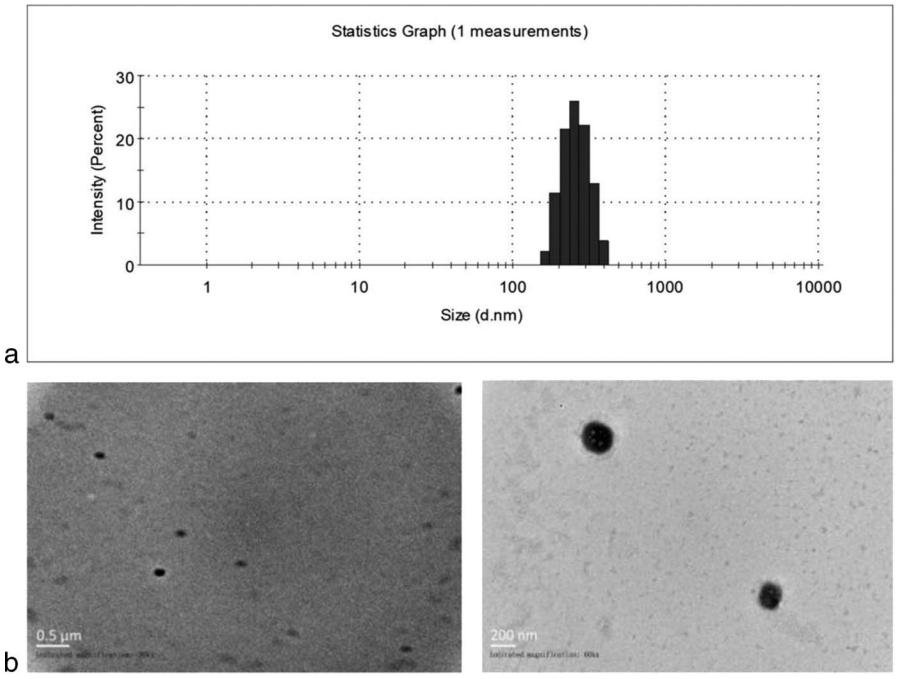

Fig. 4. (a) Hydrodynamic size distribution of CS-DPTA NP measured by DLS and (b) TEM of CS-DPTA NP (scale bar: 500 nm and 200 nm).

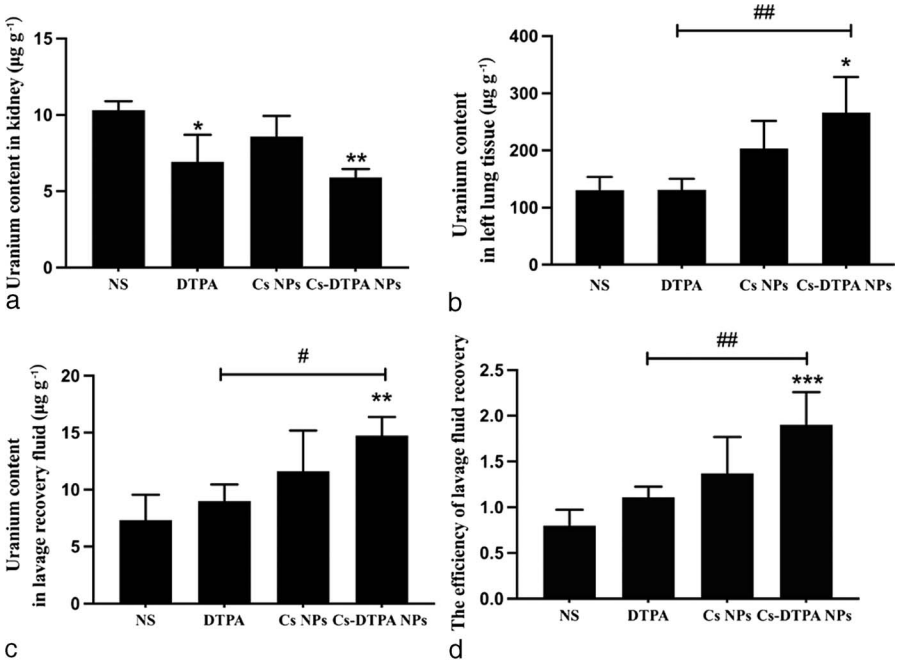

Fig. 5. Changes of U content: (a) U content in kidney tissue (n = 4), $*P < 0.05$ and $**P < 0.01$ vs. NC group; (b) U content in the lung tissues (n = 4), $*P < 0.05$ vs. NS group, $^{\#\#}P < 0.01$ vs. DTPA group; (c) U content in the lavage recovery fluid (n = 4), $^{\#}P < .05$ vs. DTPA group, $**P < .01$ vs NS group; (d) The efficiency of lavage fluid recovery (n = 4), $^{\#\#}P < 0.01$ vs. DTPA group, $***P < 0.001$ vs. NS group.

group ($P < 0.01$). Meanwhile, the DU level of the DTPA group was lower than the NS group ($P < 0.05$). Under non-lavage conditions, the U content in left lung tissues in the CS-DPTA NP group was significantly higher than the NS and DTPA groups ($P < 0.01$ and $P < 0.05$) (Fig. 5b). After lung lavage, the level of DU in the lavage fluid was compared among the groups, and the results showed that the level of DU in the lavage fluid in the CS-DPTA NP group was significantly higher than the NS and DTPA groups (Fig. 5c) ($P < 0.05$ and $P < 0.01$). The lavage recovery rate was calculated by DU content in the lavage recovery fluid. The lavage rate (100%) was calculated by DU content in the recovered lavage fluid:

$$\text{U content in the lavage fluid (100\%)} = \frac{\text{U content in the lavage fluid} \times \text{total lavage fluid volume}\left(20\,\frac{\text{mL}}{\text{kg}}\,[\text{times}]\text{animal body weight} \times 3\right) \times 100\%}{\text{total DU intake}(10\text{ mg} \times \text{animal body weight})} \quad (1)$$

The results showed that the recovery rate of lavage fluid in the CS-DPTA NP group was significantly higher than the NS and DTPA groups (Fig. 5d) ($P < 0.001$ and $P < 0.01$). The blood uranium levels in the CS-DPTA NP group increased over time after exposure to depleted uranium at 1, 3, and 7 d under non-lavage conditions and were significantly lower in 3- and 7-d lavage groups than in non-lavage group after treatments (Fig. 6). ($P < 0.05$).

Effect of CS-DPTA NP on DU induced lung inflammatory injury

After 7 d of DU exposure, specimens of lung tissue in the NS and DTPA groups showed diffused pneumonia with massive infiltration of inflammatory cells and fibrous deposits in the lung septa containing visible nodular plaques. In contrast, the inflammatory response was milder in the CS NPs and CS-DPTA NP groups (Fig. 7a). As shown in Fig. 7b, the pathology score was significantly lower in the CS-DPTA NP group than the NS group ($P < 0.05$). Based on Masson staining, the collagens were stained blue (Fig. 7c). The IL-1 of CS NPs and CS-DPTA NP groups in the lavage

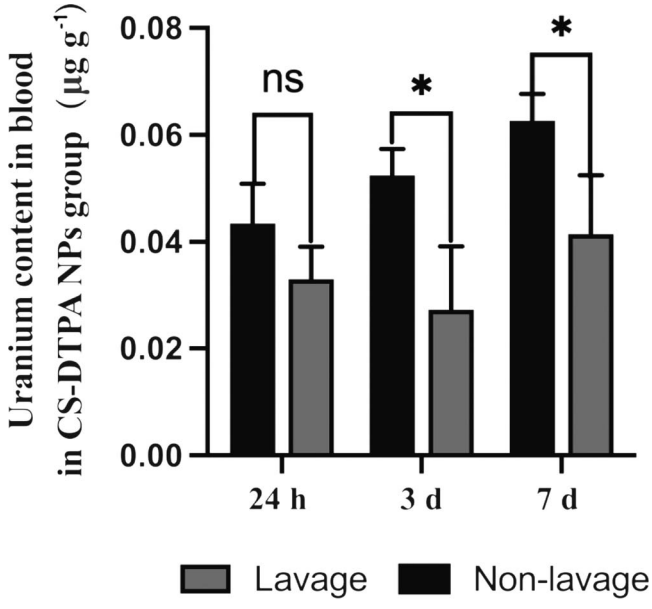

Fig. 6. U content in blood in the CS-DPTA NP group (n = 4), $*P < 0.05$.

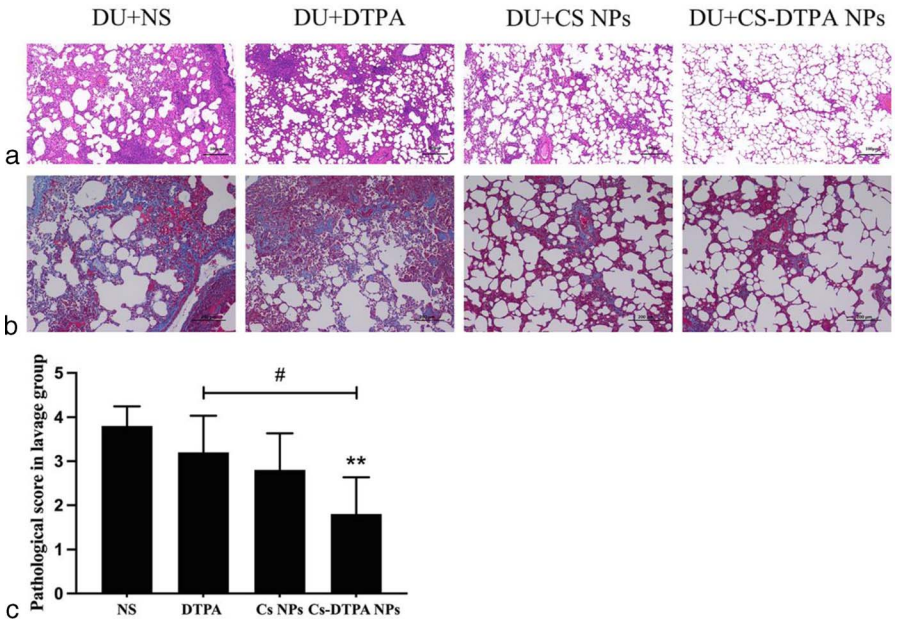

Fig. 7. Pathological changes: (a) Lung H&E staining (scale bar: 100 μm); (b) Masson staining (scale bar: 200 μm); (c) pathological score of H&E staining, $^{*}P < 0.05$ vs. NS group, $^{\#}P < 0.05$ vs. DTPA group.

fluid was significantly lower than those in the NS group ($P < 0.05$). In addition, the IL-10 and TNF-α of CS-DPTA NP were slightly lower than those in the NS and DTPA groups (Fig. 8) ($P > 0.05$).

DISCUSSION

DU weapons were developed by the US Army ever since the late 1970s (Abu-Qare and Abou-Donia 2002). With the use of DU weapons, large quantities of very small uranium

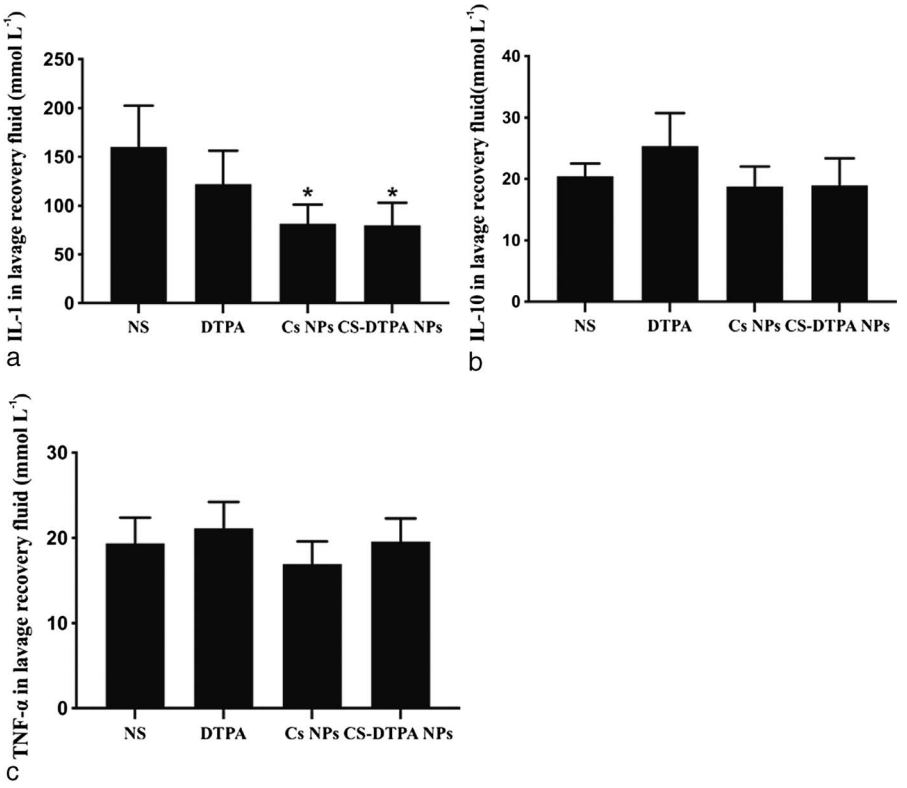

Fig. 8. Cytokine level in lavage recovery fluid: (a) IL-1; (b) TNF-α; (c) IL-10; $^{*}P < 0.05$ between two groups.

oxide dust particles were released into the environment, which can pass through the respiratory tract and reach deeply into the lungs (Xie et al. 2010). Once DU enters the lungs, it would reach the whole body. The most common and bioavailable form is the uranyl particles (UO^{2+}), which are absorbed and further form soluble complexes with bicarbonate, citrate, and proteins in the body. These particles could enter the whole body and form deposits in bones and other organs, causing long-term damage (Fattal et al. 2015). Cao et al. (2005) found that rats had to be sacrificed 4 to 14 mo after DU exposure. A large number of lymphocyte infiltrates were found in lung tissues as well as the bronchus. In addition, mucous epithelial cilia were found to be inverted, and there was a presence of pulmonary bronchitis, pulmonary hemorrhage, and lung abscesses. With an increased inhalation dose and time of DU aerosol, lung function decreased significantly. Yang (2002) found that DU was carcinogenic to human bronchial epithelial cells immortalized by adenovirus when treated with insoluble DU oxide. The absorption of DU into the blood mainly depends on its solubility. This solubility determines how quickly and efficiently the body absorbs uranium from the lungs. Soluble chemical forms are absorbed within a few days, while insoluble forms usually take months to years to be absorbed (Bleise et al. 2003). Therefore, it is particularly important to treat DU after early exposure.

In this study, a modified microfiber bronchoscopy-guided spray bronchial contamination device (Patent. No: CN201921851213.X) with positive pressure injection of insoluble DU was used to establish a simulated inhalation contamination model of insoluble DU particulate matter. Leggett (2003) found that alveolar absorption could be divided into two stages. In the first stage, U content rapidly rose, leading to a peak in plasma uranium levels. In the second stage, U content declined, followed by a long period of steady absorption. In our previous experiments, it has been confirmed that U content in the blood using this method was rapidly increased within 3 h of contamination, decreased rapidly from 3–8 h of contamination, and slowly decreased from 8 h to 1 d of contamination. The level of contamination was in a plateau phase during 1–5 d of contamination and continued to increase during 5–7 d of contamination (Fu 2021). Therefore, this model provides a good basis to investigate the effects of DU removal using different interventions.

Insoluble DU particles enter the lungs through inhalation and can remain in the lungs for a long time. These particles can also slowly dissolve into the blood, while the kidney tissue is the main target organ (Shaki et al. 2012). After glomerular filtration of uranium, it binds to the anionic site of the proximal tubular epithelial brush in the form of UO^{2+}. At the same time, it enters the cell by endocytosis, causing damage to the kidneys (Leggett 1989). Therefore, the detection of residual U content in the left lung tissue and the U content in bilateral kidneys are the most important indexes reflecting the pathological injury of the lung and kidney caused by insoluble U, and also the direct indexes indicating the intervening effects of atomized inhalation of CS-DPTA NP. The results of this study showed that the residual amount of DU under non-lavage lung conditions in lung tissues of the CS-DPTA NP group was significantly higher than that of the NS and DTPA groups ($P < 0.05$), which may be attributed to the small size and large specific surface area of CS-DPTA NP, exerting an adsorption effect on DU and making part of DU remain on the surface of lung tissue so as to provide more opportunities for later lung lavage treatment to remove residual DU. Besides, the U content in kidney tissues showed that uranium content in bilateral kidney tissues of CS-DPTA NP group and DTPA group was lower than that of the NS group. More specifically, the U content in the CS-DPTA NP group was significantly lower than the NS group ($P < 0.01$), suggesting that CS-DPTA NP could significantly reduce U accumulation in renal tissues.

Lung lavage has been considered to be the most effective approach for the removal of insoluble DU particles (Fu et al. 2021). Rump (2016) found that decontamination treatment should be provided quickly after radionuclide exposure. If delayed, an increased dose of drugs as well as longer treatment would be necessary for decontamination. Delayed treatment might also result in reduced efficacy and even had irreparable consequences. In our previous work (Fu et al. 2021), we found that the lung lavage within 3 h after respiratory exposure to radionuclides was the most effective and efficient treatment, especially when a patient inhaled insoluble dust. However, in accidental exposure to nuclear emergencies, a sufficient lung lavage in a short period is usually impossible for medical personnel. Thus, to extend the time window and guarantee the efficiency of lung lavage treatment, we propose first giving nebulized CS-DPTA NP and then performing lung lavage 24 h after exposure. As reported in this study, the insoluble DU particles in the lavage recovery fluid were significantly more in the CS-DPTA NP group than those in the NS and DTPA groups ($P < 0.05$), which was consistent with the consideration that CS-DPTA NP may adsorb some DU particles that were beneficial to lung lavage. Besides, the lavage recovery rates were 0.80%, 1.11%, 1.37%, and 1.90%, in the NS, DTPA, CS NPs, and CS-DPTA NP groups, respectively. The CS-DPTA NP group has significantly higher recovery rate of lavage fluid than the other three groups ($P < 0.05$). The lavage efficiency observed in the NS group was similar to that in a previous study for 24 h lavage, and there is still potential for the improvement of the lavage efficiency of CS-DPTA NP compared with the 3 h lavage (Fu et al. 2021). In a follow-up study, we will focus on improving lavage efficiency and accelerating the removal of insoluble DU from the lungs.

The DU concentration in blood indirectly reflects that in organs and tissues, as well as lavage efficiency (Fu 2021).

The blood U level in the CS-DPTA NP group without lavage showed a slow increasing trend at 1, 3, and 7 d of DU exposure. The insoluble DU is heavily adsorbed but slowly dissolving and releasing in the lungs. Based on this fact, damage to renal function caused by DU in the body would be continued and resulted in a lack of U excretion, showing a slow increasing trend in late blood U. The blood U levels in the lavage group at 3 and 7 d of DU exposure were significantly lower than that in the non-lavage group. We measured the blood U level before and after lavage, and there was no difference observed, proving that lavage was effective in removing intrapulmonary DU and that it did not promote the dissolution of insoluble DU.

After inhalation of insoluble DU, the U is mainly retained in the lungs and bronchial lymph nodes and could be phagocytosed by macrophages (Li 2004). Under normal conditions, inactivated macrophages have a limited ability to phagocytose and secrete cytokines. Gilberti et al. (2008) found that mouse lung macrophages engulfed in silica dust were activated and released various inflammatory mediators, leading to the accumulation of macrophages, neutrophils, and lymphocytes. The lung lavage removed insoluble DU particles from the lungs and also elicited more inflammatory factors. Results showed that IL-1 levels in the lavage fluid of the CS-DPTA NP and CS NPs groups were significantly lower than that of the NS group ($P < 0.05$). While IL-10 and TNF-α levels were not only statistically different among the four groups, these levels were also lower in the CS-DPTA NP group compared to the NS group. This may be related to anti-inflammatory properties of CS. Yoon et al. (2007) found that chitosan was able to stimulate resting-state macrophages RAW264.7 to secrete inflammatory factors and NO but also inhibits lipopolysaccharide (LPS)/IFN-activated macrophage RAW264.7 inflammatory factors and NO release.

Histopathological observations of the lung showed that the NS and DTPA groups had a large number of infiltrating inflammatory cells and septal fibrosis, as well as inflammatory nodules, with a predominance of chronic inflammation. Masson's trichrome staining revealed that collagen fiber deposition was present at greater levels in the NS and DTPA model groups compared to the CS NPs and CS-DPTA NP groups. This observation was in agreement with lung histopathological findings in lungs and also consistent with the results of deposited DU content in lung tissues.

In conclusion, we found that when CS-DPTA NPs were inhaled early during post-respiratory exposure, blocking effects on inhalation of insoluble DU particles were observed. Combined with lung lavage, the clearance efficiency of DU in lung tissues and the prognosis were both improved.

Acknowledgments—We would like to thank Li Tao for his guidance in the details of the experiment and Zhou Qing for his help in the pathology of the experiment; both individuals are from the Institute of Compound Injuries, College of Preventive Medicine, Third Military Medical University. We would like to thank CureEdit (http://wscureedit.com/) for English language editing.

The authors contributed equally to this work. This work was funded by the Military Logistics Scientific Research Key Project under Grant BLJ20J005.

REFERENCES

Abu-Qare AW, Abou-Donia MB. Depleted uranium-the growing concern. J Appl Toxicol 22:149–152; 2002. Available at ***https://pubmed.ncbi.nlm.nih.gov/12015793/***. Accessd 17 May 2002.

Andersen O. Principles and recent developments in chelation treatment of metal intoxication. Chem Rev 99:2683–2710; 1999. Available at ***https://pubmed.ncbi.nlm.nih.gov/11749497/***. Accessed 8 September 1999.

Bleise A, Danesi PR, Burkart W. Properties, use and health effects of depleted uranium (DU): a general overview. J Environ Radioact 64:93–112; 2003. Available at ***https://pubmed.ncbi.nlm.nih.gov/12500797/***. Accessed 28 May 2003.

Bosquillon C, Lombry C, Préat V, Vanbever R. Influence of formulation excipients and physical characteristics of inhalation dry powders on their aerosolization performance. J Control Release 70:329–339; 2001. Available at ***https://pubmed.ncbi.nlm.nih.gov/11182203/***. Accessed 23 February 2001.

Cao J, Cao WC, Li YP, Cheng TM, Chen JY, Cai JM, Zou F, Teng GS, Zhou LX, Li F, et al. 2014. Cheng Tianmin military preventive medicine. Beijing People's Military Medical Publishing House; 38:900–914; 2014.

Cao Z, ZM Yang Z, Sun J, Li Y. Characteristic pathological changes of main organs of rats after inhalation of depleted uranium aerosol. Chinese J Radiolog Health 2:81–84; 2005. DOI: CNKI:SUN:REDI.0.2005-02-001.

Craft E, Abu-Qare M, Flaherty M, Garofolo H, Rincavage, Abou-Donia M. Depleted and natural uranium: chemistry and toxicological effects. J Toxicol Environ Health B Crit Rev 7:297–317; 2004. Available at ***https://pubmed.ncbi.nlm.nih.gov/15205046/***. Accessed 12 August 2010.

Dean MR. An evaluation of the use of bronchopulmonary lavage in the treatment of plutonium oxide inhalation. J R Nav Med Serv 82:188–196 l 1997. Available at ***https://pubmed.ncbi.nlm.nih.gov/9167359/***. Accessed 1 January 1997.

Fattal EN, Tsapis, Phan G. Novel drug delivery systems for actinides (uranium and plutonium) decontamination agents. Adv Drug Deliv Rev 90:40–54; 2015. Available at ***https://pubmed.ncbi.nlm.nih.gov/26144994/***. Accessed 1 August 2015.

Fu W. Features of early injuries in a canine model of high dose depleted uranium exposure through bronchial spraying. J Third Military Med Univ 43:52–58; 2021. Available at 10.16016/j.1000-5404.202007210. Accessed 15 January 2021.

Fu W, Xiao Y, Zeng F, Chen X, Zhu Y, Tian Z, Liang Y, Li R, Liu M. Effect of early whole lung lavage at different time-points for promoting the removal of depleted uranium from the lung. Int J Radiat Biol 97:968–976; 2021. Available at ***https://pubmed.ncbi.nlm.nih.gov/34085887/***. Accessed 7 June 2021.

Fulco CE, Liverman CT, Sox HC. Gulf War and health: volume 1. Depleted uranium, sarin, pyridostigmine bromide, vaccines [online]. 2000. Available at ***https://pubmed.ncbi.nlm.nih.gov/25057724/***. Accessed 1 January 2000.

Gilberti RM, Joshi GN, Knecht DA. The phagocytosis of crystalline silica particles by macrophages. Am J Respir Cell Mol Biol 39:619–627; 2008. Available at ***https://pubmed.ncbi.nlm.nih.gov/18556590/***. Accessed 12 June 2008.

Gu XL, Pan XJ, Yang ZH, Liu KL, Xu L, Zhu MX. Effects of aerosol inhalation of citric acid on lung fibroblast proliferation in rats induced by depleted uranium. Chinese Pharm 23: 2313–2315; 2012. Available at 10.6039/j.issn.1001-0408.2012.25.04. Accessed 15 July 2012.

He L, LZ. Histochemical and cytochemical techniques. People's Med Pub House 2:29–41; 2014.

Hosseini SF, Soleimani MR, Nikkhah M. Chitosan/sodium tripolyphosphate nanoparticles as efficient vehicles for antioxidant peptidic fraction from common kilka. Int J Biol Macromol 111:730–737; 2018. Available at ***https://pubmed.ncbi.nlm.nih.gov/29337105/***. Accessed 18 January 2018.

Inal S, Koc E, Ulusal-Okyay G, Pasaoglu OT, Isik-Gönül I, Oz-Oyar E, Pasaoglu H, Güz G. Protective effect of adrenomedullin on contrast induced nephropathy in rats. Nefrologia 34:724–731; 2014. Available at ***https://pubmed.ncbi.nlm.nih.gov/25335086/***. Accessed 17 November 2014.

Jhaveri JZ, Raichura T, Khan M, Momin M, Omri A. Chitosan nanoparticles—insight into properties, functionalization and applications in drug delivery and theranostics. Molecules 26(2); 2021. Available at ***https://pubmed.ncbi.nlm.nih.gov/33430478/***. Accessed 7 Janunary 2021.

Leggett RW. The behavior and chemical toxicity of U in the kidney: a reassessment. Health Phys 57:365–383; 1989. Available at ***https://pubmed.ncbi.nlm.nih.gov/2674054/***. Accessed 1 September 1989.

Leggett RW, Pellmar TC. The biokinetics of uranium migrating from embedded DU fragments. J Environ Radioact 64(2–3): 205–225; 2003.

Liu Y. Study oh radiation protection of WSC-DTPA nanoparticles. J Radiat Res Radiat Process 39(5):309–315; 2012. Available at CNKI:SUN:FYFY.09 2012.05-010. Accessed 1 October 2012.

López-León T, Carvalho EL, Seijo B, Ortega-Vinuesa JL, Bastos-González D. Physicochemical characterization of chitosan nanoparticles: electrokinetic and stability behavior. J Colloid Interface Sci 283:344–351; 2005. Available at ***https://pubmed.ncbi.nlm.nih.gov/15721903/***. Accessed 15 March 2005.

Mikušová V, Mikuš P. Advances in Chitosan-based nanoparticles for drug delivery. Int J Mol Sci 22(17); 2021. Available at ***https://pubmed.ncbi.nlm.nih.gov/34502560/***. Accessed 6 September 2021.

Miller AC, Rivas R, Tesoro L, Kovalenko G, Kovaric N, Pavlovic P, Brenner D. Radiation exposure from depleted uranium: the radiation bystander effect. Toxicol Appl Pharmacol 331:135–141; 2017. Available at ***https://pubmed.ncbi.nlm.nih.gov/28602947/***. Accessed 9 June 2017.

Petitot F, Lestaevel P, Tourlonias E, Mazzucco C, Jacquinot S, Dhieux B, Delissen O, Tournier BB, Gensdarmes F, Beaunier B, Dublineau I. Inhalation of uranium nanoparticles: respiratory tract deposition and translocation to secondary target organs in rats. Toxicol Lett 217:217–225; 2013. Available at ***https://pubmed.ncbi.nlm.nih.gov/23296105/***. Accessed 4 January 2012.

Priest ND. Toxicity of depleted uranium. Lancet 357(9252):244–246; 2001. Available at ***https://pubmed.ncbi.nlm.nih.gov/11214120/***. Accessed 27 January 2001.

Ran Y, Wang S, Zhao, Li J, Ran X, Hao Y. A review of biological effects and treatments of inhaled depleted uranium aerosol. J Environ Radioact 222:106357, Available at ***https://pubmed.ncbi.nlm.nih.gov/32755761/***, Accessed 2 August 2020.

Rump A, Stricklin D, Lamkowski A, Eder S, Abend M, Port M. Reconsidering Current Decorporation Strategies after Incorporation of Radionuclides. Health Phys. 111(2):204–11. Available at https://pubmed.ncbi.nlm.nih.gov/27356066/. Accessed August 2016.

Shaki F, Hosseini MJ, Ghazi-Khansari M, Pourahmad J. Toxicity of depleted uranium on isolated rat kidney mitochondria. Biochim Biophys Acta 1820:1940–1950; 2012. Available at ***https://pubmed.ncbi.nlm.nih.gov/22940002/***. Accessed 23 August 2012.

Taylor DM. Plutonium in vivo and drugs to remove it from man. Inorganica Chimica Acta 79:43–44; 1983. Available at ***https://xueshu.baidu.com/usercenter/paper/show?paperid=2e8d1804289bfaf19be41ec3249098d2&site=xueshu_se&hitarticle=1***. Accessed 1983.

US Food and Drug Administration. Guidance for industry: calcium DTPA and zinc DTPA drug products—submitting a new drug application. Washington, DC: USFDA; 2004.

Walters EH, Gardiner PV. Bronchoalveolar lavage as a research tool. Thorax 46:613–618; 1991. Available at ***https://pubmed.ncbi.nlm.nih.gov/1948787/***. Accessed 1 September 1991.

Wang ZM, YSF. New Advances in Clinical Ultrasound Nebulized Inhalation Drugs. China Medicine Guide 9(08): 197, Available at http://www.cnki.com.cn/Article/CJFDTotal-YYXK201108148.htm. Accessed 1 May 2011.

Xie H, LaCerte C, Thompson WD, Wise JP Sr. Depleted uranium induces neoplastic transformation in human lung epithelial cells. Chem Res Toxicol 23(2):373–378, Available at ***https://pubmed.ncbi.nlm.nih.gov/20000475/***, Accessed 15 February 2010.

Yang ZH, Fan BX, Ying LU. Malignant Transformation of Human B ronchial Epithelial Cell(BEAS-2B)Induced by Depleted Uranium[J]. Chinese Journal of Cancer, 21(9):944–8. Available at http://en.cnki.com.cn/Article_en/CJFDTOTAL-AIZH200209004.htm. Accessed 1 September 2002.

Yoon HJ, Moon ME, Park HS, Im SY, Kim YH. Chitosan oligosaccharide (COS) inhibits LPS-induced inflammatory effects in RAW 264.7 macrophage cells. Biochem Biophys Res Commun 358:954–959; 2007. Available at ***https://pubmed.ncbi.nlm.nih.gov/17512902/***. Accessed 22 May 2007.

Yue YC, Li MH, Wang HB, Zhang BL, He W. The toxicological mechanisms and detoxification of depleted uranium exposure. Environ Health Prev Med 23:18; 2018. Available at ***https://pubmed.ncbi.nlm.nih.gov/29769021/***. Accessed 16 May 2018.

Zhang B, Duan YY, He H, WB H, et al. Reproduction of a model of lung injury induced by depleted uranium inhalation in canine. Medical Journal of Chinese Peoples Liberation Army, 36(2):188–191. Available at http://en.cnki.com.cn/Article_en/CJFDTOTAL-JFJY201102031.htm. Accessed 1 February 2011.

Zhang Y, Xu Y, Xi X, Shrestha S, Jiang P, Zhang W, Gao C. Amino acid-modified chitosan nanoparticles for Cu(2+) chelation to suppress CuO nanoparticle cytotoxicity. J Mater Chem B 5:3521–3530; 2017. Available at ***https://pubmed.ncbi.nlm.nih.gov/32264288/***. Accessed 21 May 2017.

Zhuang S, Zhang Q, Wang J. Adsorption of Co2+ and Sr2+ from aqueous solution by chitosan grafted with EDTA. J Molec Liquids 325:115197; 2020. Available at ***https://www.sciencedirect.com/science/article/pii/S0167732220374390***. Accessed 26 December 2020.

■■